Clin Neuroradiol (2019) 29:615–621
https://doi.org/10.1007/s00062-018-0728-7

ORIGINAL ARTICLE

Magnetic Resonance Spectroscopy Features of the Visual Pathways in Patients with Glaucoma

Direnç Özlem Aksoy[1] · Jülide Canan Umurhan Akkan[2] · Alpay Alkan[1] · Ayşe Aralaşmak[1] · Hafize Otçu Temur[1] · İsmail Yurtsever[1]

Received: 15 February 2018 / Accepted: 11 September 2018 / Published online: 5 October 2018

Abstract

Purpose The aim of the study was to investigate any metabolic changes on magnetic resonance spectroscopy (MRS) throughout the visual pathway of the brain in patients with glaucoma and a control group and correlate the results with clinical findings.

Material and Methods A total of 87 patients were enrolled in the study, 30 healthy controls, 25 glaucoma, 16 suspected glaucoma (GS) and 16 ocular hypertension (OHT) patients. A single voxel MRS on TE 30 ms was performed by placing the volume of interest (VOI) on the corpus geniculatum laterale (CGL) and primary visual cortex (VC). Peak values of metabolites, such as N-acetyl aspartate (NAA), creatine (Cr), choline (Cho) and Myo-inositol (Ins) were investigated on MRS. The MRS results were correlated with age, intraocular pressure (IOP), retinal nerve fiber length (RNFL), mean deviation (MD) and cup disk ratio (CD).

Results The NAA values obtained from the CGL in glaucoma and GS cases were lower than the healthy control group. The Cho values at CGL in glaucoma were lower than GS and controls. There was a negative correlation between NAA values of the VC and CD in glaucoma cases. Additionally, there was a negative correlation between age and RNFL in both glaucoma and GS cases.

Conclusion The use of MRS can reveal neurodegeneration in CGL and VC in patients with glaucoma. Depiction of metabolic changes throughout the visual pathways via MRS will guide the treatment planning and follow-up in glaucoma and GS cases.

Keywords Corpus geniculatum laterale (CGL) · Visual cortex (VC) · N-acetyl aspartate (NAA) · Suspected glaucoma (GS) · Open angle glaucoma

Introduction

Glaucoma is a neurodegenerative disease and one of the leading causes of vision-related morbidity in industrialized and emerging countries [1, 2]. The global prevalence of glaucoma is approximately 3.5% for people aged 40–80 years [3]. The number of people affected by glaucoma worldwide was estimated to be 64.3 million in 2013 and this number is predicted to increase to 76 million in 2020 and to 112 million in 2040 [3]. The common feature of glaucoma is slowly progressive optic nerve damage, which leads to visual field defects. As the damage caused by glaucoma is irreversible, it is important to detect it early and start treatment before patients develop significant deterioration in visual function. The neurodegenerative process can also be blamed for glaucoma pathophysiology. It is believed that degeneration affects whole parts of the visual pathways [4, 5]. It is characterized by loss of retinal ganglion cells and a reduction in the number of axons, leading to thinning of retinal nerve fiber length (RNFL) and optic nerve fibers [6, 7]. Degeneration and thickness of RNFL can be measured by optical coherence tomography (OCT) [8] but the degeneration of the posterior part of the visual pathway needs to be evaluated by advanced techniques, such as magnetic resonance imaging (MRI). The visual pathways in patients with glaucoma were evaluated with conventional MRI in a small number of studies in the literature [4, 9–11] and showed a decrease in optic nerve and visual cortex thickness

✉ Direnç Özlem Aksoy
direncozlemaksoy@gmail.com

1 Department of Radiology, Bezmialem Vakif University, 34093 Istanbul, Turkey

2 Department of Ophthalmology, Bezmialem Vakif University, Istanbul, Turkey

in glaucoma due to the neurodegenerative process in some of these studies [12–15]. In a study, which was performed with a 7 T MRI, volume loss was shown in the corpus geniculatum laterale (CGL) in glaucoma cases [9]. Other than these effects of neuronal loss, significant changes have not been identified in conventional MRI sequences. Structural and diameter changes in the neuronal tissue may not be easily noticed. Due to these reasons new and advanced neuroimaging techniques in glaucoma have recently been investigated [16, 17]. Magnetic resonance spectroscopy (MRS) is a non-invasive imaging technique, which can show early-onset brain damage and metabolic changes in various diseases where conventional MRI is within normal limits. It allows the metabolite changes in brain tissue to be determined and quantified [16].

The aim was to investigate any metabolic changes on MRS at CGL and visual cortex in patients with glaucoma and the control group and to correlate the results with clinical findings.

Material and Methods

In this study healthy controls, suspected glaucoma (GS), ocular hypertension (OHT) and open-angle glaucoma (OAG) patients were enrolled from the Glaucoma Division of the Ophthalmology Department from January 2016 to June 2017. Clinical examination findings, such as the cup disc ratio (CD), average RNFL thickness and visual field (VF) mean deviation (MD) were collected. Only one eye per patient was randomly included in the statistical analyses, unless only one eye met the inclusion and exclusion criteria. A total of 87 cases, consisting of 57 patients and 30 controls, participated in the study. The patient group was composed of 25 glaucoma (open angle glaucoma), 16 GS and 16 OHT and MR spectra were obtained from all participants. The mean age and age interval for each patient group and control group are summarized in Table 1. Ethical approval was obtained from the institutional ethical review board and all subjects provided informed consent. An informed consent form was obtained from each case.

Participants with a history of intraocular surgery (except for uncomplicated cataract surgery or glaucoma surgery), coexisting retinal pathologies, nonglaucomatous optic neuropathy, uveitis or ocular trauma were not included in the study. Participants were also not included if there was a diagnosis of Parkinson's disease, Alzheimer's disease, dementia, or a history of stroke and any condition with contraindications for MRI.

Ophthalmological Examination

At the initial evaluation, each participant underwent an ophthalmologic examination, including assessment of best corrected visual acuity (BCVA), slit-lamp biomicroscopy, intraocular pressure (IOP) measurement with Goldmann applanation tonometry, gonioscopy, ultrasound pachymetry, dilated stereoscopic examination of fundus and optic nerve head (ONH), evaluation of RNFL thickness, and visual field (VF) testing. Glaucomatous ONH morphology was defined as the presence of neuroretinal rim narrowing to the optic disc margin, notching, an increase in the c:d ratio, or RNFL defects. The RNFL thickness was measured with the Spectralis SD-OCT parapapillary circle scan (software version 5.4.7.0). Basic principles of the SD-OCT technique have been described in the literature [18]. Stan-

Table 1 Mean age and age interval for each patient group and control group

	Number of subjects	Age interval (years)	Mean age (years)
Control	30 T	30–88	49.27 ± 13.17
	13 F	33–74	45.77 ± 14.36
	17 M	38–88	51.94 ± 13.04
GS	16 T	23–62	47.19 ± 12.03
	9 F	25–57	43.44 ± 12.01
	7 M	27–62	52.00 ± 12.39
OHT	16 T	24–71	46.94 ± 10.87
	13 F	39–71	48.07 ± 11.72
	3 M	24–60	42.00 ± 13.92
Glaucoma	25 T	26–73	53.80 ± 12.04
	6 F	48–73	58.00 ± 11.63
	19 M	26–71	52.32 ± 12.36
Patients (GS + OHT + Glaucoma)	57 T	23–73	50.02 ± 11.64
	28 F	23–73	48.82 ± 11.99
	29 M	26–71	51.17 ± 12.13

GS suspected glaucoma, *OHT* Ocular hypertension, *T* Total, *F* Female, *M* Male

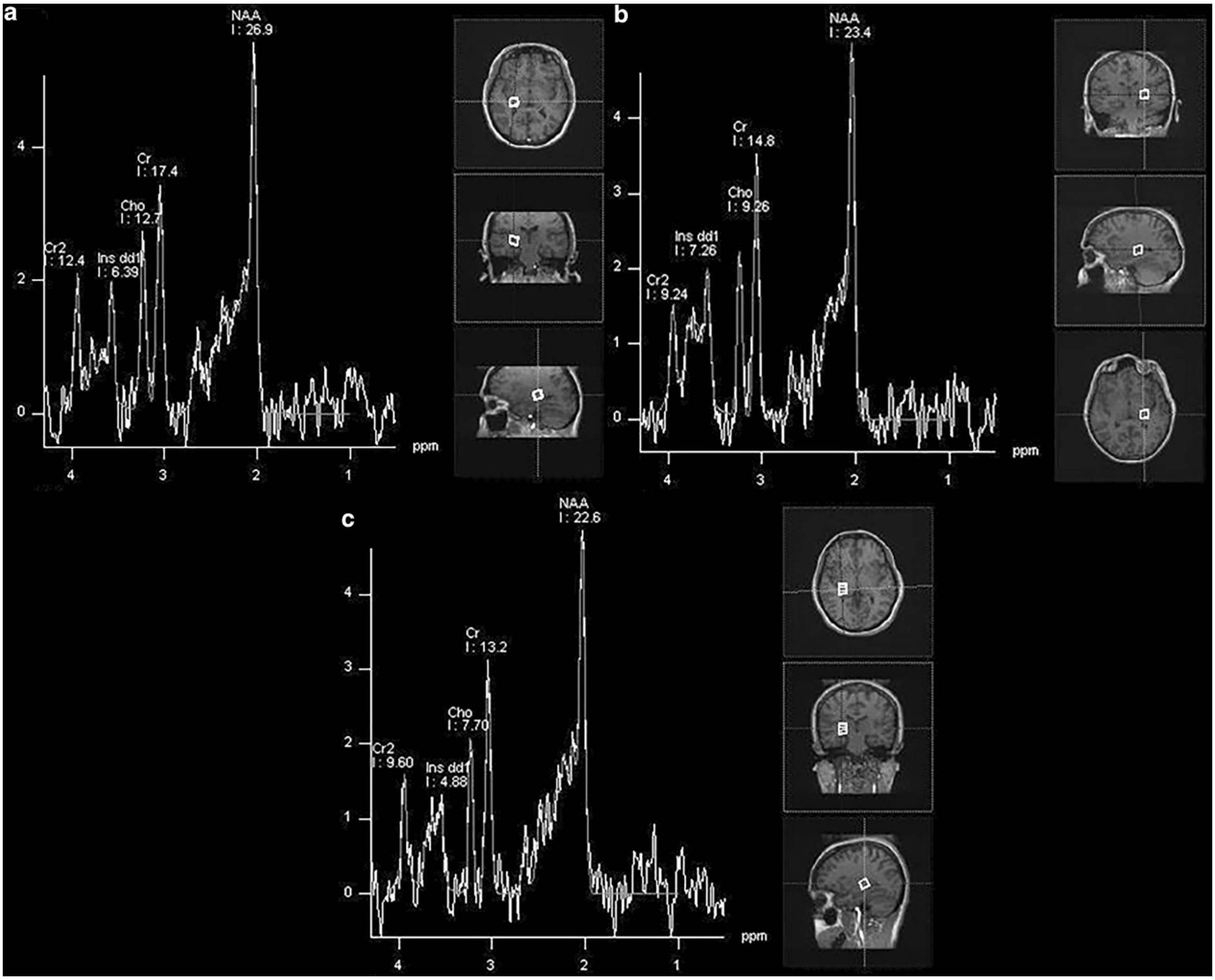

Fig. 1 Example of three distinct spectra from CGL of the control (**a**), glaucoma (**b**) and suspected glaucoma (**c**) cases in the short TE MRS examinations. The Cho and NAA values show decreased values compared to controls

dard automated perimetry (SAP) visual field tests were completed using the Swedish interactive threshold algorithm standard 24-2 (Humphrey Field Analyzer, Carl Zeiss Meditec, Dublin, CA, USA) strategies. The SAP result was considered abnormal if a glaucoma hemi-field test was outside of normal limits or a pattern standard deviation fell outside of the 95% normal confidence interval (CI). Visual field deficits were categorized according to the Hodapp-Parrish-Anderson classification [19]. Participants were classified into four groups: a healthy control group with an IOP <21 mmHg, normal ONH appearance, and normal SAP. The OHT participants were defined as having IOP >21 mmHg, normal ONH appearance, and normal SAP. Participants with glaucoma had a clinical diagnosis of primary open angle glaucoma (POAG) in at least one eye based on an IOP >21 mm Hg or more without therapy, wide anterior chamber angle, glaucomatous ONH and abnormal SAP by at least 2 reliable VF examinations. Suspected glaucoma (GS) was defined as having suspicious appearing ONH and/or IOP >21 mmHg but no VF defects on SAP. The presence of a RNFL defect was not considered as a criterion for suspicion of glaucoma. The diagnostic category for each participant was determined based on the diagnosis of the worse eye.

MRI Acquisition

In addition to clinical examination MRI data were acquired from all participants using 1.5 T scanner (Siemens, Magnetom Avanto, Erlangen, Germany) equipped with an 18-channel head coil. Axial T1-weighted (T1W) 3D gradient echo (FLASH) images of the whole brain were obtained with reconstruction of the coronal and sagittal

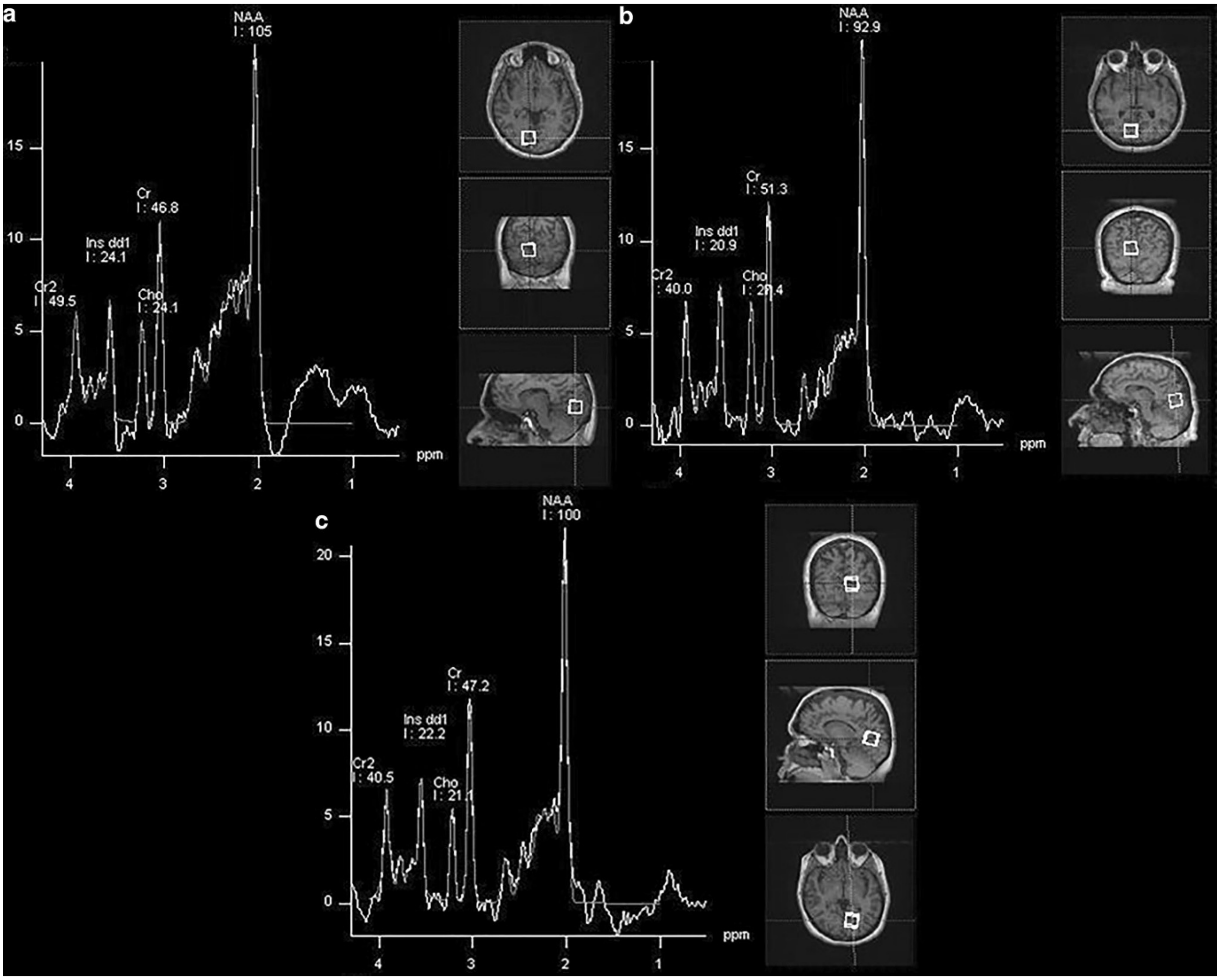

Fig. 2 MRS spectra from VC of the control (**a**), glaucoma (**b**) and suspected glaucoma (**c**) cases in the short TE MRS examinations. The Cho, Cr and NAA values show normal values

views for anatomic reference. The parameters of T1W were : TR = 8.2 ms, TE: 4.76 ms, FOV: 250 × 250 mm, matrix: 256 × 256, slice thickness: 1.0 mm, slice overlap: 0 mm, NEX: 2, FA: 20^0 with scan time: 4 min and 15s. The point resolved spectroscopy sequence (PRESS; TR/TE, 1500/30 ms) was performed. Single voxel spectroscopy was used as the MRS method. A VOI size of 13 × 13 × 13 mm^3 was placed on the anatomical localization of the CGL and 20 × 20 × 20 mm^3 on the VC. The VOI placing was confirmed based on axial, coronal and sagittal anatomical 3D T1W images. The CGL is a part of the diencephalon, which is located at the rear end of the thalamus and the first ROI for CGL was placed here. The second VOI was placed as close as possible to the posterior position of the VC. In order to standardize the localization of VOI in each case it was placed along the calcarine sulcus. Since the VOI was large, the VOI was placed to include both VC and optical radiations. Before the PRESS sequence, after placement of volume of interest (VOI) in the appropriate site, automatic shimming was performed with 3–7 Hz line width for optimum intravoxel signal and to obtain short TE single voxel spectroscopy. A 90°Gaussian pulse was applied after the spoiler gradient for water suppression. Following Fourier transformation, linear baseline values were corrected.

Data Analysis

After data acquisition, the MRS database was transferred to the workstation (Syngo MR Workstation Software Version B 17, Siemens Healthcare Solutions, Erlangen, Germany) for post-processing. With the software in the workstation, the MRS spectra are generated and the metabolites are quantified automatically. A radiologist (DÖA), who

Table 2 Metabolite values in CGL and VC for each group

	CGL				VC			
	NAA (ppm)	Cho (ppm)	Cr (ppm)	Ins (ppm)	NAA (ppm)	Cho (ppm)	Cr (ppm)	Ins (ppm)
Control	26.80 ± 4.80	10.91 ± 2.07	12.45 ± 3.55	5.21 ± 2.21	94.09 ± 37.91	27.20 ± 7.65	50.48 ± 4.15	18.03 ± 3.96
GS	20.98 ± 5.85[a]	11.75 ± 2.90	13.20 ± 3.40	4.54 ± 1.58	91.39 ± 41.88	28.44 ± 8.68	50.18 ± 7.65	15.84 ± 3.96
OHT	25.56 ± 9.66	11.17 ± 3.68	14.11 ± 9.91	4.79 ± 2.72	88.11 ± 40.27	27.22 ± 8.61	46.35 ± 10.55	14.38 ± 3.00
Glaucoma	21.18 ± 6.24[a]	9.14 ± 3.45[b]	10.21 ± 3.11	4.90 ± 1.73	81.01 ± 37.77	27.11 ± 9.81	48.26 ± 13.00	15.85 ± 4.35

CGL corpus geniculatum laterale, *VC* visual cortex, *GS* suspected glaucoma, *OHT* ocular hypertension, NAA, Cho, Cr, Ins
[a]Statistically significant when compared to controls
[b]Statistically significant when compared to GS

was blinded to the clinical data, assessed all MR spectra, received and recorded the metabolites values. Peak areas of the metabolites N-acetyl aspartate (NAA) 2 ppm, creatine (Cr) 3.02 ppm, choline (Cho) 3.2 ppm and Myo-inositol (Ins) 3.56 ppm in CGL and VC were calculated by a sum of the Gaussian curves (Figs. 1 and 2).

Statistical Analysis

Descriptive statistics are presented as mean, standard deviation and percentage. Categorical characteristics were compared with the χ^2-test. The average MRS values of the groups were compared with one-way ANOVA and post hoc Tukey HSD tests. The study also investigated whether there was any correlation between spectroscopy results and clinical examination findings. Relationships between quantitative data were evaluated by Pearson's correlation coefficient. Statistical analyses were performed with IBM SPSS 20.0 (IBM, Armonk, NY, USA). Significance level was accepted as 0.05 in all tests.

Results

Mean metabolite values of CGL and VC from the control group, glaucoma, glaucoma suspect and ocular hypertension are shown in Table 2. Mean clinical examination results, such as IOP, RNFL, MD and CD from each group are shown in Table 3 and the comparison between these groups in Table 4.

The NAA values obtained from CGL in glaucoma and GS cases were lower than the healthy control group (both $p = 0.025$, $p = 0.011$). The Cho values obtained from CGL in glaucoma were lower than GS and healthy control group. The difference of Cho values between glaucoma and GS was statistically significant ($p = 0.038$). There was a negative correlation between age and RNFL in both glaucoma ($p = 0.048$, r = –0.399) and GS ($p = 0.004$, r = –0.676). Additionally, there was a negative correlation between NAA values obtained from VC and CD in patients with glaucoma ($p = 0.049$, r = –0.397).

Discussion

Glaucoma is a specific optic neuropathy involving progressive damage to the optic nerve, deterioration of the retinal ganglion cells, and ultimately visual field loss. Glaucoma is considered to affect all visual pathways, not only leading to changes in the eyes. The visual pathway starts with retinal ganglion cells and they form optic nerve fibers, which cross into the optic chiasm to become optic tracts that consist of fibers from the other optic nerve fibers. The optic tract extends into the CGL at the thalamus. After the CGL the fibers form optic radiation that extends along to the VC. It is considered that there is anterograde and retrograde interaction in the visual pathways. There are neurotransmitters that provide back and forth transmission between retinal ganglion cells and the CGL. Some brain-derived neurotropic factors that originate from the CGL have been shown to be effective in the formation of retinal ganglion cells [20]. Often, as a trigger factor in glaucoma pathophysiology, an increase

Table 3 Clinical examination values for each patient group

		Mean ± SD
IOP	GS	17.69 ± 2.96
	OHT	23.12 ± 2.33
	Glaucoma	14.40 ± 2.43
RNFL	GS	90.19 ± 10.25
	OHT	102.94 ± 9.43
	Glaucoma	65.80 ± 12.57
MD	GS	–2.90 ± 1.88
	OHT	–0.63 ± 0.73
	Glaucoma	–10.83 ± 7.46
CD	GS	0.69 ± 0.14
	OHT	0.26 ± 0.22
	Glaucoma	0.80 ± 0.12

GS suspected glaucoma, *OHT* ocular hypertension, *IOP* intraocular pressure, *RNFL* retinal nerve fiber layer thickness, *MD* visual field mean deviation, *CD* cup disc ratio, *SD* standard deviation

Table 4 Comparison of clinical examination values for each patient group

			p-value
IOP (mmHg)	GS	OHT	0.000*
		Glaucoma	0.001*
	OHT	GS	0.000*
		Glaucoma	0.000*
	Glaucoma	GS	0.001*
		OHT	0.000*
RNFL (µm)	GS	OHT	0.006*
		Glaucoma	0.000*
	OHT	GS	0.006*
		Glaucoma	0.000*
	Glaucoma	GS	0.000*
		OHT	0.000*
MD (dB)	GS	OHT	0.423
		Glaucoma	0.000*
	OHT	GS	0.423
		Glaucoma	0.000*
	Glaucoma	GS	0.000*
		OHT	0.000*
CD	GS	OHT	0.000*
		Glaucoma	0.093
	OHT	GS	0.000*
		Glaucoma	0.000*
	Glaucoma	GS	0.093
		OHT	0.000*

GS suspected glaucoma, *OHT* ocular hypertension, *IOP* intraocular pressure; *RNFL* retinal nerve fiber layer thickness, *MD* visual field mean deviation, *CD* cup disc ratio
*$p < 0.05$

in IOP is implicated. Nevertheless, it is now accepted that the initiator is not just this but that it is a multifactorial process. The mechanism responsible for the onset and continuation of the neurodegenerative cascade is accepted as apoptosis. Different studies continue to be completed in order to detect changes in the visual pathways in glaucoma cases. White matter pathway integrity can be evaluated in the nervous system with diffusion tensor imaging (DTI). A decrease in fractional anisotropy (FA) values and an increase in mean diffusivity (MD) values were found in measurements taken from optic radiation and the optic nerve. These changes in the diffusion parameters are considered as indicative of widespread degeneration of visual pathways in glaucoma cases [11, 21, 22]. Since MRS may reflect changes in metabolites at the microstructural level it may determine early neuronal changes on the visual pathway in glaucoma cases. The use of MRS determines the numerical values of the metabolites in the area of tissue examined. The main metabolites NAA, Cr and Cho were analyzed on MRS and NAA is the indicator of the neuronal integrity. When neuronal loss occurs, a reduction in the amount of NAA is expected and Cr is necessary in energy metabolism in all cells. It is assumed that Cr is a constant metabolite and its amount does not show large changes in neurodegenerative diseases. Choline has an important role in the cell for the structure and restoration of membranes. A decrease in the value of Cho is considered a sign of deterioration of cell integrity, while an increase of value is demyelination [16, 17, 23].

The results of the MRS studies performed up to now in patients with glaucoma are controversial and a consensus has not been reached. It has been thought that apoptosis is responsible for the neurodegenerative process in glaucoma pathophysiology [23, 24]. The increase in excitatory neurotoxic substance (Glx) is attributed to the apoptosis mechanism in a few studies [23, 25]. Also it is thought that interrupting the cholinergic system due to decreased visual stimuli in glaucoma may be one of the mechanisms responsible for the pathophysiology of the neurodegenerative process. It has been shown that apoptosis may develop in the absence of Cho, which constitutes an important component of the cell membrane [26]. Chan et al. found a decrease in the Cho:Cr ratio in the visual cortex on rat models [27]. Zhang et al. argued that the fall in Cho levels might also be associated with apoptosis [17]. In this study, the Cho values of CGL in glaucoma were lower than the healthy control and GS groups. This finding may be accepted as a sign of deterioration of cell integrity and apoptosis in neuronal tissue in glaucoma cases.

Zhang et al. found a decrease in NAA/Cr ratios from the geniculocalcarine tract (GCT) and striate area of glaucoma cases in MRS [17]. The reduction in NAA levels is an indicator of neuronal loss in glaucoma. Zhang et al. argued that the low levels of NAA can only be detected during an acute attack while the degeneration process is currently taking place [17]. In this study, NAA levels in CGL were found to be lower in patients with glaucoma compared to that of controls, suggesting neuronal tissue loss in glaucoma cases. The NAA level can be used as a marker of disease process. In addition, in patients with GS, the NAA level is also found to be low in CGL. In GS cases, the low level of NAA in CGL suggests beginning of neuronal destruction, similar to cases of glaucoma. It is known that the CD increases in ophthalmologic examination in glaucoma cases and the CD is used to assess the progression of glaucoma [6]. In this study, a positive correlation was found between the increase in the CD and a decrease in the NAA value on VC in glaucoma cases. Based on this result, it is suggested that a decrease in NAA values on MRS in VC can be used to assess the progression of disease.

A limitation of the study is that one investigator placed the insertion of the VOI in the MRS examination, and it was not assessed whether there was any difference in the data obtained from the VOIs placed by different investigators on the same cases. In addition, single voxel MRS was used in this study. Both CGL and VC localizations cannot be drawn with clear boundaries therefore single voxel may not reflect the degeneration field exactly; however, the metabolite changes of the anterior visual pathways could not be evaluated. Because of the optic nerve and optic chiasm areas are small, voxels could not be placed on them.

In conclusion, MRS may reveal neurodegenerative processes and apoptosis in the optic pathway, such as CGL and VC in patients with glaucoma. Depiction of metabolic changes throughout the visual pathways by MRS may guide the treatment planning and follow-up in glaucoma.

Conflict of interest D.Ö. Aksoy, J.C.U. Akkan, A. Alkan, A. Aralaşmak, H. Otçu and İ. Yurtsever declare that they have no competing interests.

References

1. Kingman S. Glaucoma is second leading cause of blindness globally. Bull World Health Organ. 2004;82:887–8.
2. Bourne RR, Stevens GA, White RA, Smith JL, Flaxman SR, Price H, Jonas JB, Keeffe J, Leasher J, Naidoo K, Pesudovs K, Resnikoff S, Taylor HR; Vision Loss Expert Group. Causes of vision loss worldwide, 1990–2010: a systematic analysis. Lancet Glob Health. 2013;1:e339–49.
3. Tham YC, Li X, Wong TY, Quigley HA, Aung T, Cheng CY. Global prevalance of glaucoma and projections of glaucoma burden through 2040: a systematic review and meta-analysis. Ophthalmology. 2014;12:2081–90.
4. Gupta N, Ang LC, Noël de Tilly L, Bidaisee L, Yücel YH. Human glaucoma and neural degeneration in intracranial optic nerve, lateral geniculate nucleus, and visual cortex. Br J Ophthalmol. 2006;90:674–8.
5. Garaci FG, Cozzolino V, Nucci C, Gaudiello F, Ludovici A, Lupattelli T, Floris R, Simonetti G. Advances in neuroimaging of the visual pathways and their use in glaucoma. Prog Brain Res. 2008;173:165–77.
6. Jonas JB, Aung T, Bourne RR, Bron AM, Ritch R, Panda-Jonas S. Glaucoma. Lancet. 2017;309:2183–93.
7. Harwerth RS, Quigley HA. Visual field defects and retinal ganglion cell losses in patients with glaucoma. Arch Ophthalmol. 2006;124:853–9.
8. Lalezary M, Medeiros FA, Weinreb RN, Bowd C, Sample PA, Tavares IM, Tafreshi A, Zangwill LM. Baseline optical coherence tomography predicts the development of glaucomatous change in glaucoma suspects. Am J Ophthalmol. 2006;142:576–82.
9. Lee JY, Jeong HJ, Lee JH, Kim YJ, Kim EY, Kim YY, Ryu T, Cho ZH, Kim YB. An investigation of lateral geniculate nucleus volume in patients with primary open-angle glaucoma using 7 tesla magnetic resonance imaging. Invest Ophthalmol Vis Sci. 2014;55:3468–76.
10. Zikou AK, Kitsos G, Tzarouchi LC, Astrakas L, Alexiou GA, Argyropoulou MI. Voxel-based morphometry and diffusion tensor imaging of the optic pathway in primary open-angle glaucoma: a preliminary study. AJNR Am J Neuroradiol. 2012;33:128–34.
11. Garaci FG, Bolacchi F, Cerulli A, Melis M, Spanò A, Cedrone C, Floris R, Simonetti G, Nucci C. Optic nerve and optic radiation neurodegeneration in patients with glaucoma: in vivo analysis with 3-T diffusion-tensor MR imaging. Radiology. 2009;252:496–501.
12. Lagrèze WA, Gaggl M, Weigel M, Schulte-Mönting J, Bühler A, Bach M, Munk RD, Bley TA.. Retrobulbar optic nerve diameter measured by high-speed magnetic resonance imaging as a biomarker for axonal loss in glaucomatous optic atrophy. Invest Ophthalmol Vis Sci. 2009;50:4223–8.
13. Kashiwagi K, Okubo T, Tsukahara S. Association of magnetic resonance imaging of anterior optic pathway with glaucomatous visual field damage and optic disc cupping. J Glaucoma. 2004;13:189–95.
14. Ramli NM, Sidek S, Rahman FA, Peyman M, Zahari M, Rahmat K, Ramli N. Novel use of 3T MRI in assessment of optic nerve volume in glaucoma. Graefes Arch Clin Exp Ophthalmol. 2014;252:995–1000.
15. Yu L, Xie B, Yin X, Liang M, Evans AC, Wang J, Dai C. Reduced cortical thickness in primary open-angle glaucoma and its relationship to the retinal nerve fiber layer thickness. PLoS ONE. 2013;8:e73208.
16. Sidek S, Ramli N, Rahmat K, Ramli NM, Abdulrahman F, Kuo TL. In vivo proton magnetic resonance spectroscopy (1H-MRS) evaluation of the metabolite concentration of optic radiation in primary open angle glaucoma. Eur Radiol. 2016;26:4404–12.
17. Zhang Y, Chen X, Wen G, Wu G, Zhang X. Proton magnetic resonance spectroscopy (^{1}H-MRS) reveals geniculocalcarine and striate area degeneration in primary glaucoma. PLoS ONE. 2013;8:e73197.
18. van Velthoven ME, Faber DJ, Verbraak FD, van Leeuwen TG, de Smet MD. Recent developments in optical coherence tomography for imaging the retina. Prog Retin Eye Res. 2007;26:57–77.
19. Hodapp E, Parrish RK II, Anderson DR. Clinical decisions in glaucoma. St Louis: The CV Mosby Co; 1993. pp. 52–61
20. Quigley HA, McKinnon SJ, Zack DJ, Pease ME, Kerrigan-Baumrind LA, Kerrigan DF, Mitchell RS. Retrograde axonal transport of BDNF in retinal ganglion cells is blocked by acute IOP elevation in rats. Invest Ophthalmol Vis Sci. 2000;41:3460–6.
21. Zhou W, Muir ER, Chalfin S, Nagi KS, Duong TQ. MRI study of the posterior visual pathways in primary open angle glaucoma. J Glaucoma. 2017;26:173–81.
22. Zhang QJ, Wang D, Bai ZL, Ren BC, Li XH. Diffusion tensor imaging of optic nerve and optic radiation in primary chronic angle-closure glaucoma using 3T magnetic resonance imaging. Int J Ophthalmol. 2015;8:975–9.
23. Doganay S, Cankaya C, Alkan A. Evaluation of corpus geniculatum laterale and vitreous fluid by magnetic resonance spectroscopy in patients with glaucoma; a preliminary study. Eye (Lond). 2012;26:1044–51.
24. Nickells RW. Apoptosis of retinal ganglion cells in glaucoma: an update of the molecular pathways involved in cell death. Surv Ophthalmol. 1999;43:151–61.
25. Dreyer EB, Zurakowski D, Schumer RA, Podos SM, Lipton SA. Elevated glutamate levels in the vitreous body of humans and monkeys with glaucoma. Arch Ophthalmol. 1996;114:299–305.
26. Yen CL, Mar MH, Zeisel SH. Choline deficiency-induced apoptosis in PC12 cells is associated with diminished membrane phosphatidylcholine and sphingomyelin, accumulation of ceramide and diacylglycerol, and activation of a caspase. FASEB J. 1999;13:135–42.
27. Chan KC, So KF, Wu EX. Proton magnetic resonance spectroscopy revealed choline reduction in the visual cortex in an experimental model of chronic glaucoma. Exp Eye Res. 2009;88:65–70.